UNIVERSITY OF BIRMINGHAM

Research at Birmingham

Relationship of Polycyclic Aromatic Hydrocarbons with Oxy (Quinone) and Nitro Derivatives During Air Mass Transport

Harrison, Roy; Alam, Mohammed; Dang, Juan; Ismail, I.M.; Basahi, J; Alghamdi, Mansour A.; Hassan, I.A.; Khoder, M.

Link to publication on Research at Birmingham portal

1

2

3

RELATIONSHIP OF POLYCYCLIC AROMATIC HYDROCARBONS WITH OXY (QUINONE) AND NITRO DERIVATIVES DURING AIR MASS TRANSPORT

**Roy M. Harrison[1,2,3*], Mohammed S. Alam[1], Juan Dang[1‡],
I.M. Ismail[2], J. Basahi[2], Mansour A. Alghamdi[3]
I.A. Hassan[2,4] and M. Khoder[2,3]**

**[1]School of Geography, Earth and Environmental Sciences
University of Birmingham, Edgbaston, Birmingham, B15 2TT
United Kingdom**

**[2]Center of Excellence in Environmental Studies, King Abdulaziz
University, Jeddah, 21589, Saudi Arabia**

**[3]Department of Environmental Sciences, Faculty of Meteorology
Environment and Arid Land Agriculture, King Abdulaziz University
Jeddah, Saudi Arabia**

**[4]Faculty of Science, Alexandria University
21526 El Shatby, Alexandria, Egypt**

‡ Also at: Environment Research Institute, Shandong University, Jinan 250100, P.R. China
* To whom correspondence should be addressed
Tele: +44 121 414 3494; Fax: +44 121 414 3708; Email: r.m.harrison@bham.ac.uk

29 **ABSTRACT**

30 Airborne concentrations of Polycyclic Aromatic Hydrocarbons (PAH), quinone and nitro

31 derivatives have been measured at three sites on the coast of Saudi Arabia to the north of the city of

32 Jeddah. The PAH show a general reduction in concentrations from northwest to southeast,

33 consistent with a source from a petrochemical works to the northwest of the sampling sites. In

34 comparison, the concentrations of quinones show little variation between the sampling sites

35 consistent with these being predominantly longer lived secondary pollutants formed from PAH

36 oxidation. The nitro-PAH show a gradient in concentrations similar to but smaller than that for the

37 PAH suggesting a balance between atmospheric formation and removal by photolysis. The 2-

38 nitrofluoranthene:1-nitropyrene ratio increases from north to south, consistent with atmospheric

39 chemical formation of the former compound, while the ratio of 2-nitrofluoranthene:2-nitropyrene is

40 consistent with hydroxyl radical as the dominant reactant. An investigation of the changes in PAH

41 congener ratios during air mass transport along the Red Sea coast shows consistency with reaction

42 with a relatively low concentration of hydroxyl radical only for the day with the highest

43 concentrations. It is concluded that while PAH degradation is occurring by chemical reaction,

44 emissions from other locations along the air mass trajectory are most probably also leading to

45 changes in congener ratios.

46

47 **Keywords:** Polycyclic aromatic hydrocarbons; quinones; nitro-PAH; atmospheric concentrations;

48 chemical reactions.

1.   INTRODUCTION

50   Polycyclic aromatic hydrocarbons (PAH) are a group of compounds emitted widely to the

51   atmosphere from pyrolytic and petrogenic sources such as hydrocarbon fuel combustion and

52   evaporation (Ravindra et al., 2008; Harrison et al., 1996). Their atmospheric concentrations are

53   measured both in national networks and in research studies in many parts of the world. Some

54   members of the PAH group of compounds (congeners) are known human carcinogens and the

55   World Health Organization has determined an exposure-response function for cancer of the lung as

56   a result of PAH exposure, and has also reviewed other non-cancer effects upon human health

57   (WHO, 2010). The European Union has set a target value of 1 ng m^{-3} of benzo(a)pyrene as an

58   aspirational limit to minimise adverse effects upon public health.

59

60   PAH are reactive compounds and are oxidised in the atmosphere with lifetimes typically from hours

61   to days (Keyte et al., 2013). Amongst the first products of oxidation are oxy-derivatives, typically

62   quinones, and nitro derivatives. Far less is known about the carcinogenic activity of the derivatives

63   than for the PAH, but PAH quinones have been linked with reactive oxygen species (Verma et al.,

64   2015) and oxidative stress (Li et al., 2003), an important mechanism in the development of human

65   disease, and both quinones and nitro-PAH are potent *in vitro* mutagens with a consequent potential

66   to cause cancer or teratogenesis (Durant et al., 1996; Pederson and Siak, 1981).

67

68   Keyte et al. (2013) have reviewed the chemical reactivity, including mechanisms of PAH oxidation

69   and their potential for long-range transport. Walgraeve et al. (2010) reviewed the published data

70   describing oxygenated PAH in the atmosphere, including measurements of ketones,

71   carboxaldehydes, diones and quinones. Noting the relative scarcity of quinone data, Delgado-

72   Saborit et al. (2013) report measurements of 14 PAH quinones in Standard Reference Material

73   (Urban Dust) SRM1649a and SRM1649b, and in the ambient air. They compare their ambient air

74   concentration data with that from 14 other published studies. Other than for anthraquinone and

7,12-benzo(a)anthracene quinone which are reported by most studies, the majority of compounds are reported only by a sub-set of studies. Furthermore, Delgado-Saborit et al. (2013) studied the partition of quinones between the condensed and vapour phases. They found that, as for PAH, molecular weight is a good predictor of partitioning and a transition occurs in the region of molecular weight 200 to 250 from a presence predominantly in the vapour phase, to one which is mainly particle-associated, with the 50% point at molecular weight 230-240, when average air temperatures were in the range of 1-4ºC. Albinet et al., 2008 investigated the partitioning of PAH, oxy-PAH and nitro-PAH during the summer and winter seasons and noted that the partitioning of oxy-PAH and nitro-PAH were significantly different in both seasons. The 50% point at which compounds were present in the vapour and condensed phase increased in the summer from a molecular weight of 180-190 to 200-210 for oxy-PAH and 190-200 to 210-220 for nitro-PAH, confirming that temperature may have an influence in the partitioning. Data for nitro-PAH in the atmosphere are scarce in the literature, with very few studies reporting concentrations of a few compounds (e.g. Albinet et al., 2007; Ringuet et al., 2012; Souza et al., 2014; Dimashki et al., 2000).

In this study, concentrations of PAH, quinones and nitro-derivatives have been measured during summer and winter periods at three sites in Saudi Arabia and the concentration data and inter-relations between compounds are reported in this paper. The spatial distribution of the PAH has been discussed in an earlier paper (Harrison et al., 2016), where it was concluded that the emissions from the large petrochemical works at Yanbu to the northwest of Rayes could be responsible for the observed spatial distribution and congener profile of PAH.

2.   AIR SAMPLING AND ANALYSIS

The air sampling sites and protocols used in this work have been reported by Harrison et al. (2016), and a map of the sampling locations appears in Figure 1. Particulate and vapour forms of the PAH

4

101 and their derivatives were sampled separately onto quartz filters and a PUF substrate respectively

102 using a Tisch "pesticide" sampler with a TSP inlet. Samples were collected over 24-hour periods,

103 offset by 6 hours between samples, commencing at Rayes, with sampling 6 hours later at Rabegh

104 and a further 6 hours later at Abhur.

105

106 Quartz filters were cleaned prior to use by heating at 400ºC, followed by storage in a sealed

107 container. PUF substrates were cleared by ultrasonification in dichloromethane (200 mL) at 20ºC

108 for 30 minutes. These were stored in sealed bags in a -18ºC freezer. After use in the field, filters

109 and PUF substrates were wrapped in cleaned aluminium foil, sealed in plastic bags and stored at

110 -18ºC. The extraction, clean-up and preparation of samples prior to analysis incorporated a solid

111 phase extraction step developed from methods described previously (Albinet et al., 2006; Cochran

112 et al., 2012). Briefly, samples were spiked with a known amount of p-terphenyl-d14 (>99% purity,

113 Greyhound Chromatography, Merseyside, UK) and 1-fluoro-7-nitrofluorene (>98% purity, Sigma-

114 Aldrich Company Ltd., Gillingham, UK) as recovery standards for PAH and OPAH/NPAH,

115 respectively. Filters were placed inside a glass flask and spiked with internal standard (IS) mixture

116 (deuterated PAH, NPAH and OPAH compounds (>98% purity, Sigma-Aldrich Company Ltd.,

117 Gillingham, UK)). Approximately 15 mL DCM (HPLC grade, >98% purity, Fisher Scientific UK

118 Ltd) was added and the flask was covered with aluminium foil to prevent any evaporative loss of

119 analyte and/or standard. PUF substrates were placed and compressed inside a large glass beaker,

120 spiked with IS mixture. Approximately 300 mL DCM was added to each PUF substrate.

121

122 Filters and PUF substrates were extracted by ultrasonication at 20°C for 30 minutes. Due to the

123 larger volume of solvent used for PUF substrate extractions, samples were initially transferred to

124 Turbovap apparatus (biotage Ltd, Uppsala, Sweden) and blown down under a gentle stream of

125 nitrogen to reduce sample volume to approximately 5mL, prior to sample clean up. Extracted

126 samples were passed through a Pasteur pipette containing 1g anhydrous sodium sulphate (Sigma-

5

127 Aldrich Company Ltd., Gillingham, UK), concentrated under a gentle stream of nitrogen to almost

128 dryness and then made up to 1mL with hexane (HPLC grade, >98% purity, Fisher Scientific UK

129 Ltd).

130

131 Sample extracts were then subject to a solid phase extraction step, based on the methodology

132 described by Cochran et al., (2012). An aminopropyl solid phase extraction tube (Sigma-Aldrich

133 Company Ltd., Gillingham, UK) was pre-eluted with 3x 1mL aliquots of DCM followed by the

134 same measure of hexane. The sample was then passed through the column and target compounds

135 were eluted by the sequential DCM/hexane solvent gradient (3 x 1mL) of 20/80%, 35/65%,

136 50/50%. This resulted in optimum recovery of PAH, NPAH and OPAH compounds in one sample

137 extract to undergo analysis for PAH and OPAH/NPAH separately. Extracts were further reduced

138 under nitrogen to almost dryness and made up to a final volume of 100 µL with nonane (HPLC

139 grade, >98% purity, Fisher Scientific UK Ltd), ready for analysis.

140

141 Sixteen PAH, listed in Table 1 were analysed using Gas Chromatography (Agilent 6890) on a non-

142 polar capillary column (Agilent HP-5MS, 30 m, 0.25 mm ID, 0.25 µm film thickness – 5%

143 phenylpolysiloxane) coupled to a quadrupole mass spectrometer (Agilent 5973N). Detection limits

144 lay below 1 pg m^{-3} for all compounds, and precision was $8 \pm 4\%$, and accuracy (defined as the

145 difference between the measured and true value as a percentage of the true value) was $6 \pm 4\%$

146 (Delgado-Saborit et al., 2010). Analysis of NIST SRM 1649b was used to quality assure the

147 measurements.

148

149 Quinone and nitro-PAH compounds were analysed using Gas Chromatography (Agilent 6890W) on

150 a Restek Rxi-PAH column (60 m, 0.25 mm ID, 0.1 µm film thickness) coupled to an Agilent 5973

151 MSD operated in negative ion chemical ionisation (NICI) and SIM mode, as in Alam et al., (2015).

152 We demonstrated good agreement of our measurements with values reported for NIST SRM 1649b

153   (as in Delgado-Saborit et al., 2013). Some of the PUF substrates were found to be contaminated in

154   the high molecular weight (five to seven rings) region, making quantification uncertain.

155   Concentrations expressed are therefore only for the particle phase of these compounds, but the error

156   is likely to be no more than ca. 10% (Alghamdi et al., 2015; Delgado-Saborit et al., 2013).

157

158   As site details are important to the interpretation of these data, these are given below:

159

160   **Site C (Abhur) (21.7572ºN; 39.1147ºE)** is located in the grounds of a research institute on the Red

161   Sea coast to the west of major roads. It is in the northern suburbs of the major city of Jeddah

162   (population 5 million), with the King Abdulaziz international airport to the east (inland). The site is

163   approximately 130 km to the SE of Rabegh.

164

165   **Site D (Rabegh) (22.8122ºN; 39.0664ºE)** is a site located about 1 km from the residential areas of

166   this substantial city, which has appreciable local industry. The sampling site is ca. 500 metres east

167   of the coastal road. It is approximately 100 km SSE of Rayes.

168

169   **Site E (Rayes) (23.5756ºN; 38.6058ºE)** is a sparsely developed area with little road traffic and no

170   appreciable local sources. The sampling site is located about 950 metres inland (east) of the coastal

171   road, and 25-50 km SSE of the large industrial complex in the region of Yanbu.

172

173   **3.   RESULTS AND DISCUSSION**

174   Polycyclic aromatic hydrocarbons (PAH) are reactive in the atmosphere with lifetimes typically of a

175   few hours for the most reactive congeners, and a few days for the least. Ratios of compounds can

176   change dramatically during atmospheric transport as a result of differential reactivity. Alam et al.

177   (2013) have interpreted differences in concentration ratios between roadside and urban background

178   sites in terms of differential reactivity of congeners. Compounds of low reactivity showed only a

179 small elevation in concentration at the roadside site, while the more reactive compounds show

180 larger ratios due to loss in the more aged air sampled at the background site. Using a similar

181 approach, Alam et al. (2014) studied ratios between congeners measured in urban air, and those

182 sampled in rural air. The urban/rural ratios were found to be greatest for the more reactive

183 compounds, and in air masses which had aged most during atmospheric transport.

184

185 Concentrations of PAH measured in this study have been discussed by Harrison et al. (2015) and

186 will not be considered further. The measured concentrations of the parent PAH, quinones and nitro-

187 PAH appear in Table 1, and ranges of comparative data from the literature appear in Tables 2 and 3.

188 There are large divergences between published studies seen in Tables 2 and 3 for the sampled

189 compounds, which are seen clearly when individual studies are identified in Tables S1 and S2

190 (Supplementary Information). These may arise from strongly differing degrees of local pollution,

191 or interferences in the analytical procedure. These are challenging trace analyses, and hence

192 analytical artefacts are a very real possibility. However, the concentrations measured in our work

193 (Table 1) appear broadly consistent with those published previously (Tables S1 and S2). The PAH

194 concentrations have been discussed in relation to other published data by Harrison et al. (2016).

195

196 In addition to mean concentration, Table 1 includes the percentage particulate phase (%P). As is

197 normally seen in PAH datasets, there is a strong trend of increasing percentage particulate phase

198 with molecular weight, with three ring compounds being almost wholly vapour, while the

199 compounds with five or more rings are predominantly particulate. This trend has been reported

200 previously in samples collected in Jeddah, Saudi Arabia by Alghamdi et al. (2015). Similar

201 behaviour is seen also in the quinones (as noted previously by Delgado-Saborit et al., 2013) and

202 nitro-PAH (see Table 1).

203

204

3.1   Quinone: Parent PAH Ratios

Alam et al. (2014) also studied quinone:parent PAH ratios, finding a relationship to air mass age. In winter, ratios of phenanthraquinone to phenanthrene (PQ:PHE) in the UK were highest in the most aged air masses with origins in the arctic, with some values in the range 1.0-1.2, although some lower values were also present. In the less aged air from mainland Europe and the United Kingdom, ratios were lower, almost all falling below PQ/PHE = 0.4. In the present work, winter ratios were mostly in the range from <0.1-0.6, and in summer samples ranged up to 1.3. Hence the two datasets appear broadly consistent, although the period of ageing of the emissions in the Saudi Arabian air masses is likely to be much smaller, provided the PAH are emitted in the vicinity of Yanbu as Harrison et al. (2016) hypothesise. In the work of Alam et al. (2014) in the UK, ratios of anthraquinone to anthracene (AQ:ANT) in winter were again higher in the more aged air masses mostly in the range of 1.0-1.8. In the less aged air masses winter ratios of AQ:ANT ranged from 0.2-0.7. In summer, in the more aged arctic air, AQ:ANT was generally higher than in the winter with all data in the range of 1.1-1.8 and in the less aged air was 0.2-0.8. In the Saudi Arabian air masses, AQ/ANT was much higher with ratios ranging from 1.2-33.8. The other ratio reported by Alam et al. (2014) was for benzo(a)anthracene-7,12-quinone which showed winter ratios to benzo(a)anthracene from 0.2-1.4 (BaAQ:BaA) with ratios in the more aged air masses generally >1.0, but always <1.0 in the less aged air. Ratios in the Saudi Arabian dataset ranged from <0.1-4.6. From this comparison, we infer that the ratios for PQ:PHE and BaAQ:BaA are broadly comparable in the current dataset from Saudi Arabia to that from the UK reported by Alam et al. (2014).

It is noteworthy that the rate coefficient for oxidation of anthracene by the hydroxyl radical is a factor of 5.1 times greater than that of phenanthrene. Consequently if the processing time were shorter in Saudi Arabia as would be consistent with transport of emissions arising from the Yanbu petrochemical works, but the hydroxyl radical concentrations were greater, then higher AQ:ANT

9

231 ratios than PQ:PHE ratios would be expected, and are observed. Due to higher sunlight intensity

232 and hence more rapid ozone photolysis, combined with higher absolute water vapour concentrations

233 in the Saudi atmosphere, higher concentrations of hydroxyl radical are to be expected. At a

234 representative hydroxyl radical concentration of 2×10^6 cm^{-3}, the atmospheric lifetime (time taken

235 to reduce concentration by 1/e) of anthracene is around one hour, whereas that for phenanthrene is

236 around 5.5 hours. The travel time for the air mass from Yanbu to Rayes is of the order of 2-3 hours.

237 It should be remembered that the samples were collected over 24-hour periods and hence include

238 nighttime when reactions will have been much slower than during daytime. Although nocturnal

239 reactions with the NO_3 radical are possible (Keyte et al., 2013), their rate is very uncertain without

240 knowledge of the concentration either of NO_3 itself, or of its precursor NO_2.

241

242 **3.2   Seasonal Variations in Ratios**

243 Walgraeve et al. (2010) reviewed quinone:parent PAH ratios from various parts of the world,

244 reporting that during winter, 50% of ratios fell between 0.006 and 0.16. On the other hand, in

245 summer, ratios were typically 20-fold higher, with 50% lying between 0.54 and 3.6.

246

247 Ratios between quinones and their parent PAH were scrutinised for seasonal differences (see also

248 discussion above). Compounds showing a marked elevation in quinone:PAH ratio in the summer

249 samples were anthraquinone and phenanthraquinone, while ratios for other quinones,

250 acenaphthoquinone to acenaphthene, 2-methylanthraquinone and 2,3-dimethylanthraquinone to

251 anthracene did not show obvious seasonal differences. The quinone:PAH ratio may be viewed as

252 reflecting the relative stability of the parent PAH and quinone to oxidation. The oxidative capacity

253 of the atmosphere is expected to be greater in summer than winter, and those compounds for which

254 quinone/parent PAH ratios are elevated in summer seem likely to be those for which the quinone is

255 more resistant to oxidation than the parent PAH.

256

257   Some contrasting behaviour was seen in the nitro-PAH compounds. The compounds 1-

258   nitronaphthalene, 2-nitronaphthalene, 1-nitrofluoranthene, 2-nitrofluoranthene and 1-nitropyrene

259   showed higher concentrations in winter than summer. These compounds include some which arise

260   predominantly from primary emissions and others largely resulting from atmospheric chemical

261   reactions of PAH. The nitro-PAH are subject to atmospheric decay by photolysis

262   (Phousongphouang and Arey, 2003; Feilberg et al., 1999; Reisen and Arey, 2005) and hence it

263   might be expected to find higher concentrations when sunlight is less intense, unless more rapid

264   formation via a photochemically driven pathway outweighs this. Not only were concentrations of

265   nitro-PAH higher in the winter, ratios of 9-nitroanthracene:anthracene, 1-

266   nitrofluoranthene:fluoranthene, 2-nitrofluoranthene:fluoranthene, 1-nitropyrene:pyrene, 2-

267   nitropyrene:pyrene, and 6-nitrochrysene:chrysene, were all higher in the winter samples.

268

269   **3.3   Spatial Variation of Concentrations**

270   As seen in Figure 2 there was remarkable similarity in the concentrations measured at all three sites

271   for anthraquinone, and phenanthraquinone, and between Rabegh (Site D) and Rayes (Site E) there

272   was quite close agreement for acenaphthoquinone, 2-methyl-anthraquinone, 2,3-

273   dimethylanthraquinone and benzo(a)anthracene-7,12-dione. The Coefficient of Divergence (COD),

274   defined in Harrison at al. (2016) is a measure of spatial uniformity of concentrations. It takes values

275   between zero (total uniformity) and one (totally divergent). In all cases, the COD (see Table 4) was

276   below 0.3, and in the closest case (phenanthraquinone and anthraquinone between Rabegh and

277   Rayes) was <0.1. This level of agreement was much higher than for the PAH concentrations. Also

278   in the case of 1,5-dinitronaphthalene, 9-nitroanthracene, 1-nitrofluoranthene, 2-nitrofluoranthene

279   and 7-nitrobenzo(a)anthracene the COD was <0.3 for Rabegh and Rayes, showing moderate

280   agreement. This high degree of spatial uniformity is typically seen for secondary pollutants such as

281   sulphate, which are formed slowly in the atmosphere, and are subject to sink processes working on

282   a long timescale. Rates of sulphur dioxide oxidation to form sulphate are typically only about 1-3%

11

283   per hour, far slower than the comparatively very rapid oxidation processes of the predominantly

284   vapour phase PAH, such as anthracene and phenanthrene. It would appear that the lifetimes of the

285   quinones are far greater than those of the parent PAH, or they would show far greater spatial

286   dependence than is actually observed. Following this line of argument, it appears that the lifetimes

287   of the majority of nitro-PAH would probably be intermediate between those of the PAH (short) and

288   quinones (long). The increase in quinone:PAH ratios with atmospheric transport seen by Alam et

289   al. (2013; 2014) and in this work is consistent with quinones having greater stability than the parent

290   compound.

291

292   **3.4   Spatial Transformation of PAH and Derivatives**

293   As outlined by Harrison et al. (2016), who show an example trajectory, there were 14 days on

294   which the air mass arriving at Abhur had followed the Red Sea coast from the northwest. As some

295   data were missing, data were averaged for a sub-set of 4 days with complete data, and a coastal

296   trajectory. Figure 2 shows (a) the average PAH, (b) average quinones, and (c) average nitro-PAH

297   concentrations at the three sites over these days. The average travel time of the air mass between

298   sites E (Rayes) and C (Abhur) was estimated as 9.5 hours. Figure 2(a) shows a substantial decline

299   in the concentrations of all PAH, which could be the result of dilution with cleaner air, or chemical

300   reactions, or more probably a combination of the two. The quinones (Figure 2(b)) show much

301   greater spatial uniformity, reflected in low coefficients of divergence (Table 4(a)), probably

302   reflecting their largely secondary nature (although there is an important primary component) and

303   suggesting appreciable longevity. It is clear that the PAH loss between sites seen in Figure 2(a) is

304   not converted to any substantial degree into quinone, or there would be larger inter-site differences

305   seen in Figure 2(b). The nitro-PAH do show greater spatial variation (Figure 2(c) and Table 4(b)).

306   Most nitro-PAH have a primary component, and the spatial differences seen in Figure 2(c) may

307   reflect dilution of primary emitted material. This, however, seems unlikely. If the major upwind

308   source is a petrochemical plant, vapour loss is likely to be the largest PAH source and this would

12

309 contain PAH, but not the quinones and nitro-PAH which are combustion products. Consequently,

310 nitro-PAH are more probably reflective of reaction products, and their concentrations reflect a

311 balance between formation and loss, the latter predominantly by photolysis (Phousongphouang and

312 Arey, 2003; Feilberg et al., 1999; Reisen and Arey, 2005).

313

314 Ratios between nitrofluoranthene and nitropyrene compounds can be indicative of atmospheric

315 processes. Specifically, the 2-nitrofluoranthene:1-nitropyrene ratio (2-NF/1-NP) is indicative of the

316 relative contribution of atmospheric reactions via OH and NO_3 relative to direct emissions (Keyte et

317 al., 2013). A ratio >5 can be taken as indicative of atmospheric reactions, while a ratio <5 is more

318 likely to reflect direct emissions. Mean site ratios in this study varied between 1.98 at site E and

319 5.38 at site C (Table 5) indicating contributions from both sources. It is notable that the ratio rises

320 monotonically from site E (Rayes) to site C (Abhur) showing an increasing influence of

321 atmospheric chemical formation. The ratio of 2-nitrofluoranthene:2-nitropyrene (2-NF/2-NP) can be

322 diagnostic of the relative importance of OH and NO_3 radicals in oxidising PAH. A value of

323 between 5-10 indicates dominance of the OH reaction, while those of >100 reflect an important

324 contribution of NO_3 radical attack on the aromatic compound (Keyte et al., 2013). In this study,

325 ratios remained close to 5 (see Table 5), suggesting that the OH radical is the more important

326 reactant. For identical concentrations of fluoranthene and pyrene, the yield ratio for OH reaction is

327 2-nitrofluoranthene:2-nitropyrene = 6, which is close to our observed values. This is similar to that

328 observed by Alam et al. (2015) in Birmingham, UK.

329

330 **3.5   Decay Rates of PAH**

331 With the exception of acenaphthene which reacts rapidly with ozone, the atmospheric degradation

332 of PAH is primarily by reaction with the hydroxyl radical (Keyte et al., 2013). Rate coefficients are

333 available for the reaction of the vapour of low molecular weight PAH with the hydroxyl radical,

334 hence allowing prediction of their atmospheric decomposition. The use of such decay rates is

335   however difficult to relate to decay during transport in the atmosphere since a plume containing

336   PAH will be subject to dilution and potentially to the introduction of fresh emissions. In the case of

337   the three sites to the north of Jeddah (Rayes, Rabegh and Abhur), there are relatively few PAH

338   sources and the possibility exists that the plume from the Yanbu petrochemical works would travel

339   to the southeast with relatively little injection of fresh pollutant. Since PAH react at very different

340   rates with the hydroxyl radical, the ratios between congeners should change in a consistent manner

341   irrespective of absolute concentrations which are affected by dilution processes. The concept was

342   tested by application of the following equation which describes the change of PAH ratios as a

343   function of their relative rates of reaction with the hydroxyl radical:

344

345 $$\ln([PAH_i]_t/[PAH_j]_t) = \ln([PAH_i]_0/[PAH_j]_0) + [OH](k'(g)OH - k(g)OH)t$$

346   where $[PAH_i]_t$ and $[PAH_j]_t$ are the final concentrations of PAH congeners i and j after reaction time

347   (t), $[PAH_i]_0$ and $[PAH_j]_0$ are the initial concentrations of PAH congeners, [OH] is an estimated

348   hydroxyl concentration, and $k(g)OH$ and $k'(g)OH$ are the OH reaction rate coefficients for PAH_i and

349   PAH_j, respectively. It is assumed that the compounds considered in the calculation are wholly in

350   the vapour phase, as only a very small proportion of the low molecular weight compounds is in the

351   condensed phase (Alghamdi et al., 2015 and Table 1). It is also assumed that loss by deposition is

352   similar for both compounds.

353
354   The unknown in the equation is the hydroxyl radical concentration which can be output from the

355   calculation, and can be compared with measured or modelled values giving a valuable check on the

356   likelihood that the concentration changes seen are consistent with this reaction.

357
358   For periods with appropriate air mass back trajectories, the ratios of PAH congeners (fluorene,

359   phenanthrene, anthracene, fluoranthene and pyrene) were used in the above equation for a source

360   site (Rayes or Rabegh) and a receptor site (Rabegh or Abhur) and a travel time estimated from the

361   air mass back trajectory calculated using HYSPLIT. The results of this calculation were in many

362 cases inconsistent with the congener ratios changing due solely to reaction with the hydroxyl radical

363 except in the case of 29th September which was the date with the highly elevated concentrations

364 which are shown for the three sites in Figure 3. For this date, the various combinations of sites and

365 congener ratios led to broadly consistent estimates of hydroxyl radical concentration (24-hour

366 mean) and a typical value calculated from concentration of phenanthrene and anthracene at Rayes

367 and Abhur is 3.4×10^5 cm^{-3}. This is low in relation to what might be anticipated as a hydroxyl

368 radical concentration for rural Saudi Arabia based upon published data. Bahm and Khalil (2004)

369 estimate September zonally averaged OH concentrations at 0.5km altitude and 25°N as 2.6×10^6

370 cm^{-3}. They comment that the Spivakovsky model (Spivakovsky et al., 2000) and MOZART-1

371 model (Brasseur et al., 1998; Hauglustaine et al., 1998) estimate lower OH over land near the

372 surface. An important consideration, however, is that a release of PAH from the petrochemical

373 works is likely to have been accompanied by much greater concentrations of other volatile organic

374 compounds whose effect on the concentration of hydroxyl radical is difficult to predict as many

375 would act as a sink, although the cycling of OH through peroxy radical chemistry may well also be

376 promoted. This effect cannot be quantified without measurements of concentrations of VOC and

377 NO$_x$, and a chemistry-transport model, or direct OH measurements.

378

379 Our inference is that the concentrations measured on 29th September are consistent with the decay

380 of PAH by reaction with a relatively low concentration of hydroxyl radical; however, data for the

381 other days could not be fitted with this model suggesting that emissions of PAH from intermediate

382 sites on the air mass trajectory introduced fresh pollutant hence changing congener ratios from those

383 which would have prevailed in the absence of such emissions.

384

385 The data in Table 1 has been scruitinised to look for any consistent shift in the % particulate which

386 would be indicative of a preferential reaction of either the vapour or condensed phase of the PAH

387 (Keyte et al, 2013). No obvious pattern of behaviour is seen in Table 1 which is unsuprising as PAH

15

388 repartition actively between the phases in response to changing temperature or concentrations

389 within a phase, in order to restore the phase equilibrium.

390

391 **4.   CONCLUSIONS**

392 The spatial distribution of PAH and their nitro- and oxy- derivatives have been demonstrated

393 through sampling at three sites on the Red Sea coast of Saudi Arabia. The PAH show greater

394 spatial variability than either the oxy derivatives (quinones) or nitro-PAH reflecting their greater

395 chemical reactivity. The more abundant quinone compounds show a high degree of spatial

396 uniformity consistent with their presence primarily as secondary pollutants, and the ratio of

397 quinones to parent PAH increases with distance from the probable major source of PAH which is a

398 petrochemical works to the northwest of the sampling locations. The concentrations of PAH decline

399 monotonically from northwest to southeast as air masses travel along the Red Sea coast, which is a

400 result both of chemical degradation and atmospheric dilution. The influence of chemical reactions

401 has been assessed through the evaluation of changing ratios of compounds of different reactivity,

402 which inherently controls for concentration changes due to dilution. Using the assumption that the

403 breakdown of PAH is due to the reaction with hydroxyl radical, concentrations of hydroxyl have

404 been calculated from the changing PAH ratios and estimated travel time of air masses between the

405 sampling sites. In general the calculations do not yield realistic values for OH except for one day,

406 29th September 2013, when higher PAH concentrations were observed. However the calculated OH

407 radical concentration is significantly lower than the prediction of global models, which maybe due

408 to emissions of VOC and NO_x acting as a sink for OH or may be due to other sources of PAH

409 emissions influencing concentrations between the source and receptor sites. However the results

410 illustrate that atmospheric transport of PAH across a sparsely populated desert area is accompanied

411 by an atmospheric breakdown rate broadly consistent with anticipated free radical concentrations.

412 On other days, it appears likely that PAH emitted between the upwind and downwind sites has a

413 sufficient influence upon the ratio to make the calculation unworkable.

414 **5.**   **ACKNOWLEDGEMENTS**

418

419 **REFERENCES**
420

421 Alam, M.S., Delgado-Saborit, J.M., Stark, C., Harrison, R.M., 2013. Using atmospheric
422 measurements of PAH and quinone compounds at roadside and urban background sites to assess
423 sources and reactivity. Atmos. Environ. 77, 24-35.

424

425 Alam, M.S., Delgado-Saborit, J.M., Stark, C., Harrison, R.M., 2014. Investigating PAH relative
426 reactivity using congener profiles, quinone measurements and back trajectories. Atmos. Chem.
427 Phys. 14, 2467-2477.

428

429 Alam, M.S., Keyte, I.J., Yin, J., Stark, C., Jones, A.M., Harrison, R.M., 2015. Diurnal variability of
430 polycyclic aromatic compound (PAC) concentrations: Relationship with meteorological conditions
431 and inferred sources. Atmos. Environ. 122, 427-438.

432

433 Albinet, A., Leoz-Garziandia, E., Budzinski, H., ViIlenave, E., 2006. Simultaneous analysis of
434 oxygenated and nitrated polycyclic aromatic hydrocarbons on standard reference material 1649a
435 (urban dust) and on natural ambient air samples by gas chromatography-mass spectrometry with
436 negative ion chemical ionisation. J. Chromat. A. 1121, 106-113.

437

438 Albinet, A., Leoz-Garziandia E., Budzinski, H., Villenave, E., 2007. Polycyclic aromatic
439 hydrocarbons (PAHs), nitrated PAHs and oxygenated PAHs in ambient air of the Marseilles area
440 (South France): Concentrations and sources. Sci. Total Environ. 384, 280-292.

441

442 Albinet, A., Leoz-Garziandia, E., Budzinski, H., Villenave, E., Jaffrezo, J.L., 2008. Nitrated and
443 oxygenated derivatives of polycyclic aromatic hydrocarbons in the ambient air of two French alpine
444 valleys – part 1: concentrations, sources and gas/particle partitioning. Atmos. Environ. 42, 43-54

445

446 Alghamdi, M.A., Alam, M.S., Yin, J., Stark, C., Jang, E., Harrison, R.M., Shamy, M., Khoder, M.I.,
447 Shabbaj, I.I., 2015. Receptor modelling study of polycyclic aromatic hydrocarbons in Jeddah,
448 Saudi Arabia. Sci. Tot. Environ. 506-507, 401-408.

449

450 Bahm, D., Khalil, M.A.K., 2004. A new model of tropospheric hydroxyl radical concentrations.
451 Chemosphere 54, 143-166.

452

453 Brasseur, G.P., Hauglustaine, D.A., Walters, S., Rasch, P.J., Muller, J.-F., Grainer, C., Tie, X.X.,
454 1998. MOZART, a global chemical transport model for ozone and related chemical tracers. 1.
455 Model description. J. Geophys. Res 103, 28265-28289.

456

457 Cochran, R.E., Dongari, N., Jeong, H., Beranek, J., Haddadi, S., Shipp, J., Kubatova, A., 2012.
458 Determination of polycyclic aromatic hydrocarbons and their oxy-, nitro-, and hydroxy-oxidation
459 products. Analytica Chimica Acta. 740, 93-103.

460

461 Delgado-Saborit, J.M., Aquilina, N., Baker, S., Harrad, S., Meddings, C., Harrison, R.M., 2010.
462 Determination of atmospheric particulate-phase polycyclic aromatic hydrocarbons from low volume
463 air samples. Anal. Methods 2, 231-242.

464

465 Delgado-Saborit, J.M., Alam, M.S., Godri, K.J., Stark, C., Harrison, R.M., 2013. Analysis of
466 atmospheric concentrations of quinones and polycyclic aromatic hydrocarbons in vapour and
467 particulate phases. Atmos. Environ. 77, 974-982.

468

469 Dimashki, M., Harrad, S., Harrison, R.M., 2000. Measurement of nitro-PAH in the atmospheres
470 of two cities. Atmos. Environ. 34, 2459-2469.

471 Durant, J.L., Busby Jr, W.F., Lafleur, A.L., Penman, B.W., Crespi, C.L., 1996. Human cell
472 mutagenicity of oxygenated, nitrated and unsubstituted polycyclic aromatic hydrocarbons
473 associated with urban aerosols. Mutat. Res. 123-157.
474
475 Feilberg, A., Kamens, R.M., Strommen, M.R., Nielsen, T., 1999. Photochemistry and partitioning
476 of semivolatile nitro-PAH in the atmosphere. Polycycl. Aromat. Comp. 14 & 15, 151-160.
477
478 Harrison, R.M., Smith, D.J.T. and Luhana, L. 1996. Source apportionment of atmospheric
479 polycyclic aromatic hydrocarbons collected from an urban location in Birmingham, UK, Environ.
480 Sci. Technol. 30, 825-832.
481
482 Harrison, R.M., Alam, M.S., Dang, J., Basahi, J., Alghamdi, M.A., Ismail, I.M., Khoder, M.,
483 Hassan, I.A., 2016. Influence of petrochemical installations upon PAH concentrations at sites in
484 western Saudi Arabia. Atmos. Pollut. Res. in press.
485
486 Hauglustaine, D.A., Brasseur, G.P., Walters, S., Rasch, P.J., Muller, J.-F., Emmons, L.K., Carroll,
487 M.A., 1998. MOZART, a global chemical transport model for ozone and related chemical tracers.
488 2. Model results and evaluatin. J. Geophys. Res. 103, 28291-28335.
489
490 Keyte, I.J., Harrison, R.M. and Lammel, G., 2013. Chemical reactivity and long-range transport
491 potential of polycyclic aromatic hydrocarbons - A review. Chem. Soc. Rev. 42, 9333-9391.
492
493 Li, N., Sioutas, C., Cho, A., Schmitz, D., Misra, C., Sempf, J., Wang, M., Oberley, T., Froines, H.,
494 Nel, A., 2003. Ultrafine particulate pollutants induce oxidative stress and mitochondrial damage.
495 Environ. Health Perspect. 111, 455.
496
497 Pederson, T.C., Siak, J.-S., 1981. The role of nitroaromatic compound sin the direct-acting
498 mutagenicity of diesel particle extracts. J. Appl. Toxicol. 1, 54-60.
499
500 Phousongphouang, P.T., Arey, J., 2003. Rate constants for the photolysis of the nitroaphthalenes
501 and methylnitronaphthalenes. J. Photochem. Photobiol. A: Chemistry 157, 301-309.
502
503 Ravindra, K., Sokhi, R. and Van Grieken, R., 2008. Atmospheric polycyclic aromatic
504 hydrocarbons: Source attribution, emission factors and regulation. Atmos. Environ. 42, 2895-
505 2921.
506
507 Reisen, F., Arey, J., 2005. Atmospheric reactions influence seasonal PAH and Nitro-PAH
508 concentrations in the Los Angeles Basin. Environ. Sci. Technol. 39, 64-73.
509
510 Ringuet, J., Leoz-Garziandia, E., Budzinski, H., Villenave E., Albinet A., 2012. Particle size
511 distribution of nitrated and oxygenated polycyclic aromatic hydrocarbons (NPAHs and OPAHs) on
512 traffic and suburban sites of a European megacity: Paris (France). Atmos. Chem. Phys. 12, 8877-
513 8887.
514
515 Souza, K.F., Carvalho, L.R.F., Allen, A.G., Cardoso, A.A., 2014. Diurnal and nocturnal
516 measurements of PAH, nitro-PAH, and oxy-PAH compounds in atmospheric particulate matter of a
517 sugar cane burning region. Atmos. Environ. 83, 193-201.
518
519 Spivakovsky, C.M., Logan J.A., Montzka, S.A., Balkanski, Y.J., Foreman-Fowler, M., Jones,
520 D.B.A., Horowitz L.W., Fusco, A.C., Brenninkmeijer, C.A.M., Prather, M.J., Wofsy, S.C.,
521 McElroy, M.B., 2000. Three-dimensional climatological distribution of tropospheric OH: Update
522 and evaluation. J. Geophys, Res. 105, 8931-8980.

523 Verma, V., Wang, Y., El-Afifi, R., Fang, T., Rowland, J., Russell, A.G., Weber, R.J., 2015.
524 Fractionating ambient humic-like substances (HULIS) for their reactive oxygen secies activity –
525 Assessing the importance of quonones and atmospheric aging. Atmos. Environ. 120, 351-359.
526
527 Walgraeve, C., Demeestere, D., Dewulf, J., Zimmermann, R., Van Langenhove, H., 2010.
528 Oxygenated polycyclic aromatic hydrocarbons in atmospheric particulate matter: molecular
529 characterization and occurrence. Atmos. Environ. 44, 1831-1846.
530
531 WHO, 2010. WHO Guidelines for Indoor Air Quality: Selected Pollutants, World Health
532 Organization, Regional Office for Europe, Copenhagen, Denmark.
533
534
535

Table 1: Total concentrations of PAH, quinone, and nitro-PAH compounds and percentage in the particulate phase at Abhur (site C), Rabegh (site D) and Rayes (site E) (ng m^{-3}).

PAH Congener	Site C				Site D				Site E			
	Mean	Range	Number of samples	Mean P%	Mean	Range	Number of samples	Mean P%	Mean	Range	Number of samples	Mean P%
Fluorene	0.47	0.20-1.54	10	1.8%	0.91	0.45-1.92	15	0.7%	1.13	0.36-6.98	22	0.9%
Phenanthrene	6.03	2.57-12.09	10	3.1%	7.74	4.51-14.41	15	2.0%	9.58	3.24-29.92	22	1.9%
Anthracene	0.31	0.14-0.79	10	4.5%	0.40	0.20-1.30	15	2.8%	0.82	0.19-7.53	22	2.4%
Fluoranthene	0.94	0.50-1.67	10	6.3%	1.20	0.69-2.53	15	4.5%	1.18	0.40-5.86	22	5.9%
Pyrene	0.89	0.43-1.50	10	7.5%	1.44	0.79-2.51	15	3.9%	1.11	0.27-7.08	22	7.2%
Retene	0.56	0.05-1.14	10	16.0%	0.49	0.16-1.09	15	5.3%	0.52	0.21-1.75	22	8.6%
Benzo(a)anthracene	0.26	0.05-0.59	10	27.6%	0.39	0.04-1.00	15	21.0%	0.37	0.02-1.48	22	30.0%
Chrysene	0.26	0.07-0.47	10	60.4%	0.30	0.02-0.61	15	54.4%	0.39	0.06-1.91	22	47.7%
Benzo(b)fluoranthene	0.12	0.01-0.25	19	88.1%	0.16	0.05-0.25	22	85.8%	0.23	0.04-1.53	22	78.2%
Benzo(k)fluoranthene	0.12	0.02-0.23	19	90.3%	0.16	0.02-0.25	22	86.5%	0.24	0.04-2.08	22	84.7%
Benzo(e)pyrene	0.10	0.01-0.27	19	100.0%	0.11	0.02-0.29	22	100.0%	0.19	0.03-1.68	22	100.0%
Benzo(a)pyrene	0.07	0.01-0.16	19	100.0%	0.09	0.01-0.14	22	100.0%	0.16	0.01-1.53	22	100.0%
Indeno(1,2,3-cd)pyrene	0.09	0.01-0.17	19	100.0%	0.09	0.02-0.29	22	100.0%	0.18	0.03-1.89	22	100.0%
Dibenz(a,h)anthracene	0.03	0.01-0.08	19	100.0%	0.04	0.01-0.12	22	100.0%	0.08	0.01-0.67	22	100.0%
Benzo(ghi)perylene	0.11	0.02-0.32	19	100.0%	0.18	0.04-0.69	22	100.0%	0.24	0.04-2.32	22	100.0%
Coronene	0.09	0.03-0.21	19	100.0%	0.16	0.04-0.45	22	100.0%	0.20	0.06-1.54	22	100.0%
Quinone Congener												
1,4-Naphthoquinone	0.00	0.00-0.01	19	100.0%	n.d.	n.d.	22	n.d.	n.d.	n.d.	22	n.d.
2-Methyl-1,4-naphthoquinone	0.12	0.02-0.41	19	100.0%	0.10	0.05-0.14	22	100.0%	0.11	0.01-0.26	22	100.0%
Acenaphthoquinone	9.14	1.70-23.30	10	0.2%	10.89	2.44-25.62	15	9.6%	6.61	2.84-11.31	22	12.6%
Anthraquinone	3.31	0.44-8.37	10	3.9%	4.02	0.80-9.33	15	19.0%	3.15	0.76-8.92	22	16.9%
Phenanthraquinone	2.31	0.31-5.93	10	5.7%	2.86	0.57-7.35	15	18.6%	2.34	0.52-8.25	22	16.4%
2,6-Di-tert-butyl-1,4-benzoquinone	1.43	0.91-2.32	10	6.8%	1.99	1.19-4.74	15	28.5%	1.78	0.71-3.54	22	27.7%
2-Methyl-anthraquinone	0.17	0.05-0.81	10	44.6%	0.52	0.13-0.82	15	81.4%	0.42	0.07-0.93	22	79.8%
2,3-Dimethyl-anthraquinone	0.18	0.12-0.27	10	80.2%	0.38	0.14-0.64	15	91.8%	0.36	0.10-0.80	22	91.9%

Benz(a)anthracene-7,12-dione	0.11	0.01-0.20	19	100.0%	0.05	0.01-0.11	22	100.0%	0.07	0.02-0.37	22	100.0%
5,12-Naphthacenequinone	0.11	0.02-0.20	19	100.0%	0.07	0.01-0.41	22	100.0%	0.09	0.00-0.42	22	100.0%
NPAH Congener												
1-Nitronaphthalene	5.62	1.55-18.82	10	2.0%	6.70	1.43-23.13	15	1.2%	3.98	0.45-13.84	22	2.0%
2-Nitronaphthalene	4.88	1.37-15.65	10	6.6%	4.77	1.60-15.39	15	4.8%	2.41	0.33-7.03	22	5.8%
1,5-Dinitronaphthalene	0.78	0.26-1.57	10	50.9%	0.82	0.44-1.63	15	47.4%	1.07	0.58-1.79	22	52.5%
9-Nitroanthracene	0.61	0.35-1.11	10	56.7%	0.56	0.21-1.08	15	56.0%	0.65	0.24-1.71	22	56.2%
1-Nitrofluoranthene	0.13	0.01-0.57	19	91.7%	0.15	0.02-0.50	22	93.0%	0.23	0.08-0.54	22	91.7%
2-Nitrofluoranthene	0.78	0.13-2.39	19	86.0%	0.50	0.12-1.27	22	89.2%	0.59	0.08-3.32	22	88.5%
1-Nitropyrene	0.34	0.01-2.03	19	89.0%	0.55	0.01-4.23	22	87.5%	0.61	0.06-4.24	22	89.9%
2-Nitropyrene	0.16	0.02-0.44	19	88.6%	0.13	0.02-0.61	22	91.9%	0.23	0.03-1.71	22	93.7%
7-Nitrobenzo(a)anthracene	0.56	0.01-2.49	19	100.0%	0.47	0.10-1.32	22	100.0%	0.53	0.10-1.85	22	100.0%
6-Nitrochrysene	0.06	0.01-0.16	19	100.0%	0.06	0.01-0.19	22	100.0%	0.1	0.01-0.19	22	100.0%

n.d. = not determined

Table 2: Range of concentrations of PAH quinones reported in the literature.

Compound	Concentration (ng m^{-3})
9,10 phenanthrenequinone	0.01 – 2.0
5,12-naphthacenequinone	0.02 – 1.6
1-acenaphthenone	0.01 – 0.45
1,4-naphthoquinone	0.02 – 1.03
Anthracene-9,10-dione	0.056 – 13
2-methylanthraquinone	0.05 – 1.31
Benz(a)anthracene-7,12-dione	0.012 – 1.0
2,3-dimethylanthraquinone	0.04 – 0.54

Table 3: Range of concentrations of nitro-PAH reported in the literature.

Compound	Concentration (pg m^{-3})
1-Nitronaphthalene	0.2 - 700
2-Nitronaphthalene	0.0 - 292
1,5-Dinitronaphthalene	No data
2-Nitrofluorene	0 – 100
9-Nitroanthracene	9 – 846
1-Nitrofluoranthene	0.01 – 0.19[+]
2-Nitrofluoranthene	11.7 – 1700
3-Nitrofluoranthene	0.28 - 250
4-Nitropyrene	0 – 2.9
1-Nitropyrene	1 – 222
7-Nitrobenz(a)anthracene	0.7 – 130
6-Nitrochrysene	0.1 – 148
2-Nitropyrene	0.8 – 60
1,3-Dinitropyrene	0.1 – 1.2
1,6-Dinitropyrene	0 – 0.1
1,8-Dinitropyrene	0.3 – 8.7

[+] Sum of particulate plus vapour phases

**Table 4:** Coefficients of divergence (COD) values for (a) oxy-PAHs; (b) nitro-PAHs.

(a)

Species	$COD_{A\&Rg}$	$COD_{A\&Rs}$	$COD_{Rg\&Rs}$
1,4-Naphthoquinone	1.000	0.964	/
2-Methyl-1,4-naphthoquinone	0.349	0.444	0.294
Acenaphthoquinone	0.257	0.224	0.255
Anthraquinone	0.195	0.177	0.101
Phenanthraquinone	0.195	0.185	0.098
2,6-Di-tert-butyl-1,4-benzoquinone	0.270	0.247	0.134
2-Methyl-anthraquinone	0.628	0.575	0.216
2,3-Dimethyl-anthraquinone	0.409	0.425	0.168
Benz(a)anthracene-7,12-dione	0.446	0.377	0.250
5,12-Naphthacenequinone	0.441	0.435	0.343

(b)

| Species	$COD_{A\&Rg}$	$COD_{A\&Rs}$	$COD_{Rg\&Rs}$
1-Nitronaphthalene	0.260	0.415	0.381
2-Nitronaphthalene	0.292	0.480	0.422
1,5-Dinitronaphthalene	0.219	0.332	0.226
9-Nitroanthracene	0.135	0.145	0.156
1-Nitrofluoranthene	0.337	0.457	0.335
2-Nitrofluoranthene	0.302	0.450	0.328
1-Nitropyrene	0.309	0.519	0.421
2-Nitropyrene	0.365	0.471	0.404
7-Nitrobenzo(a)anthracene	0.392	0.396	0.291
6-Nitrochrysene	0.299	0.465	0.451

Note: A = Abhur ; Rg = Rabegh ; Rs = Rayes

Table 5: Range and mean of ratios at C (Abhur), D (Rabegh) and E (Rayes) sites for nitrofluoranthene (NF) and nitropyrene (NP) isomers.

| Ratios	Site C		Site D		Site E	
	Mean	Range	Mean	Range	Mean	Range
2-NF/1-NP	5.38	0.16-11.18	2.82	0.07-9.38	1.98	0.08-6.56
2-NF/2-NP	4.78	2.11-7.40	4.49	1.02-9.19	3.91	0.94-14.12
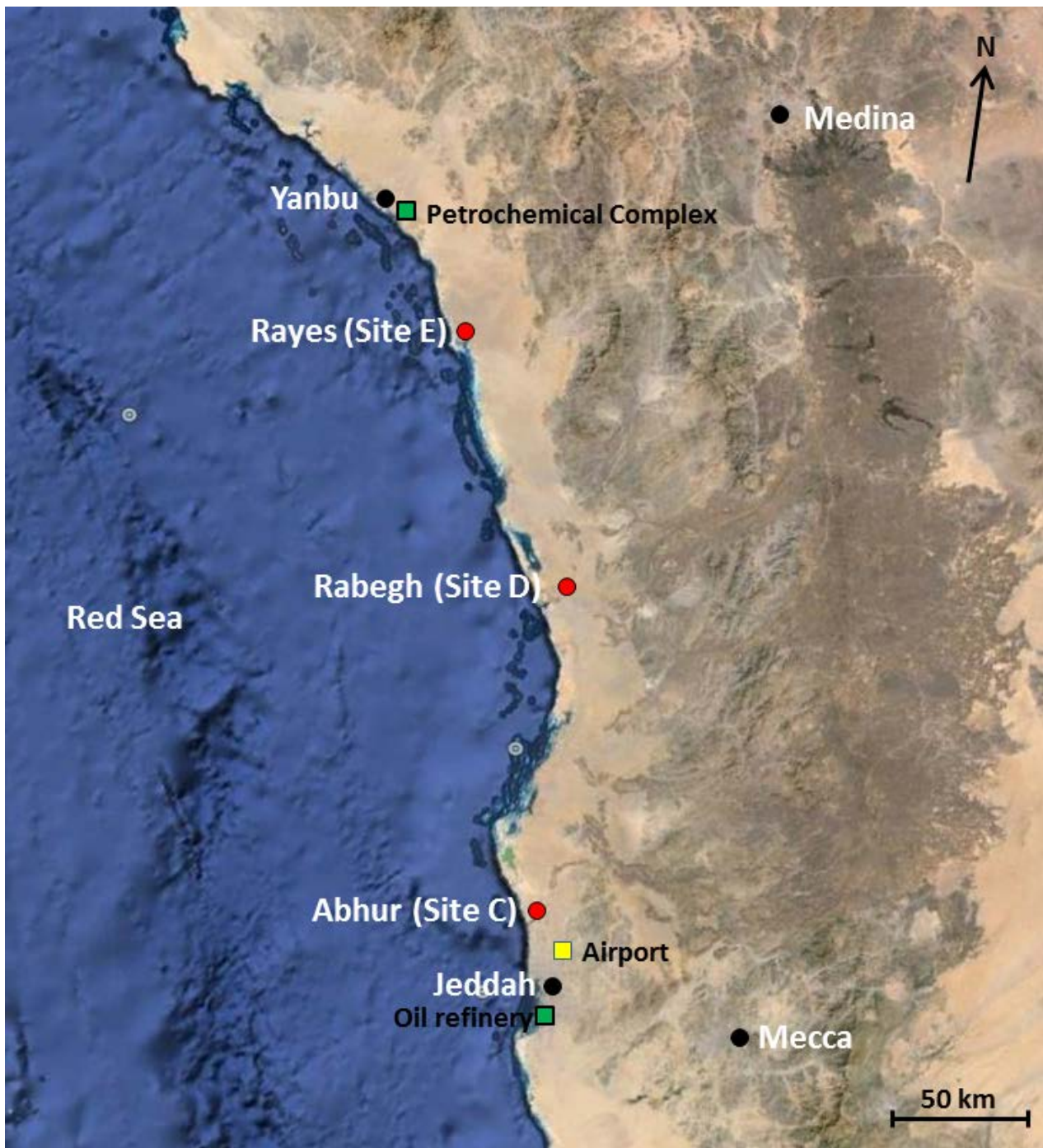
Figure 1: Locations of sampling sites and the city of Jeddah. The sites are: C Abhur; D-Rabegh and E-Rayes. Sites A and B are within Jeddah.
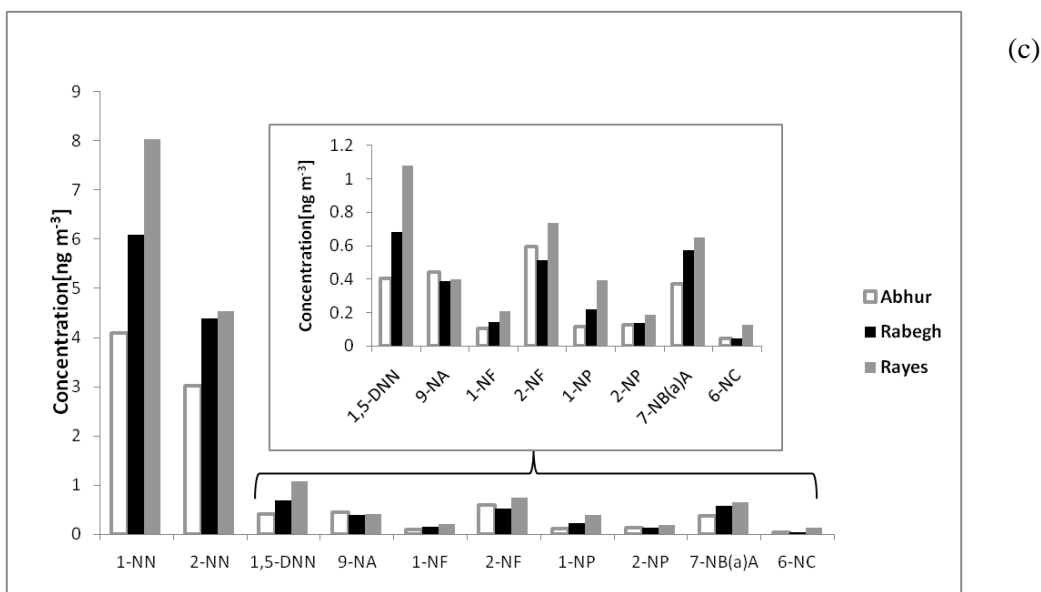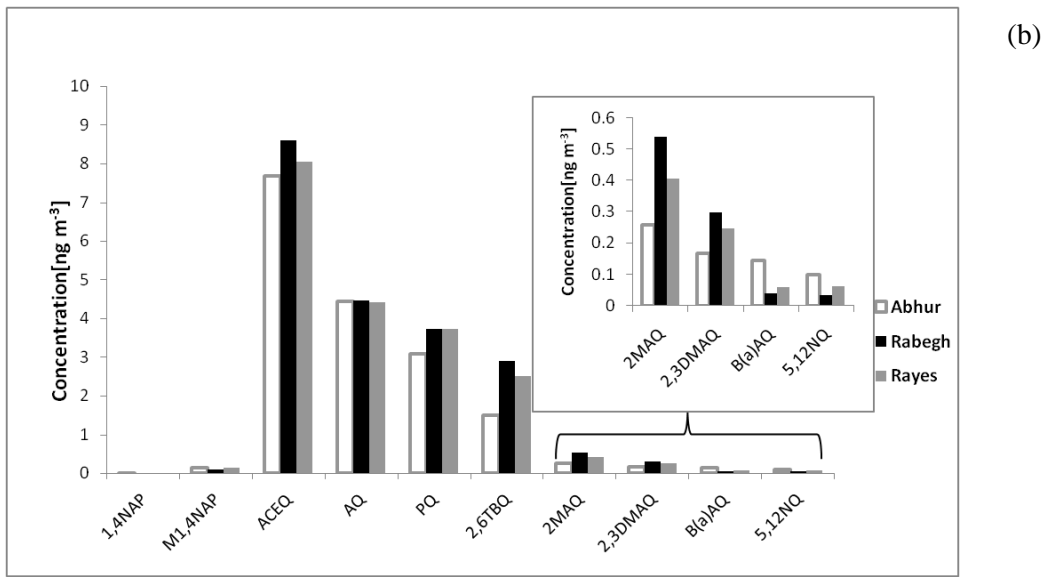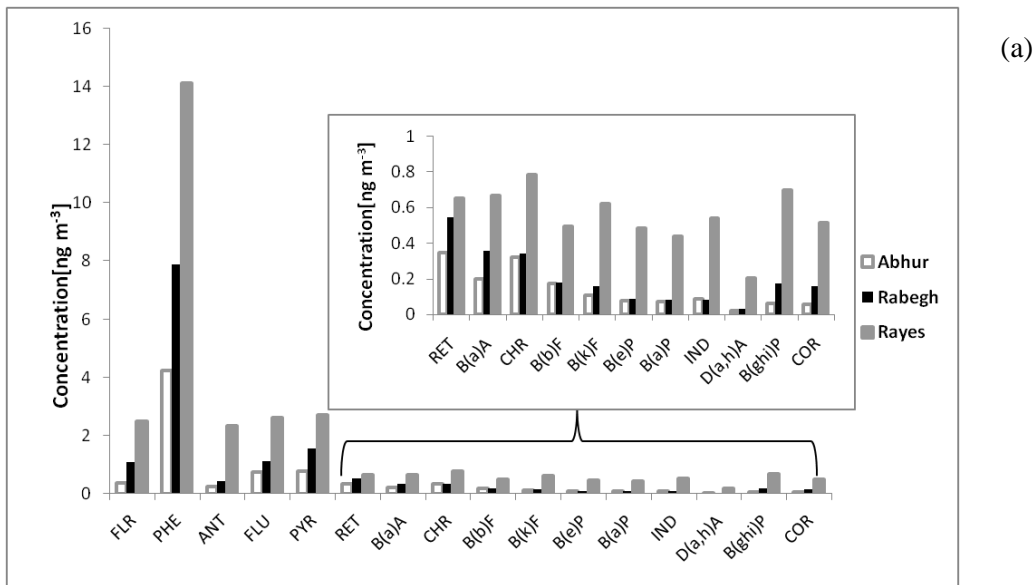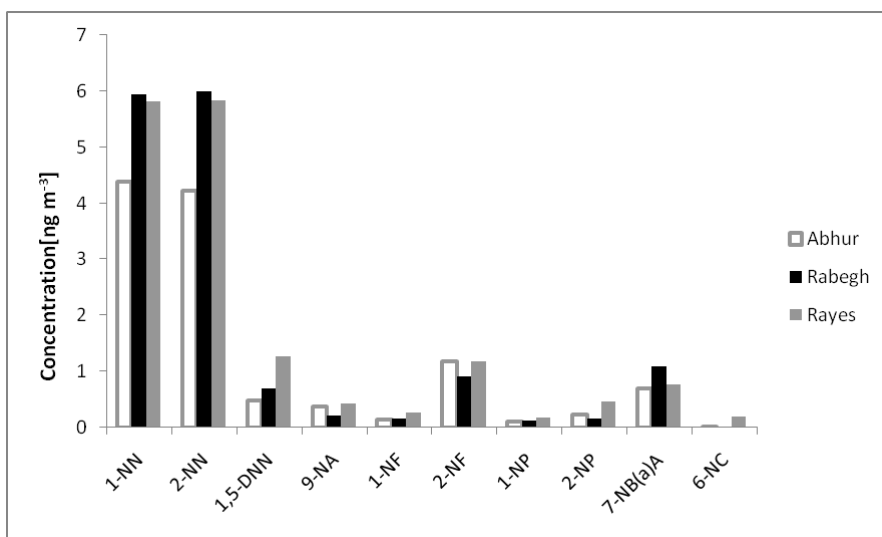
Figure 2: (a) Total PAH; (b) total oxy-PAH and (c)total nitro-PAH averaged over 4 days on which the air travelled from northwest to southeast following the Red Sea coast.
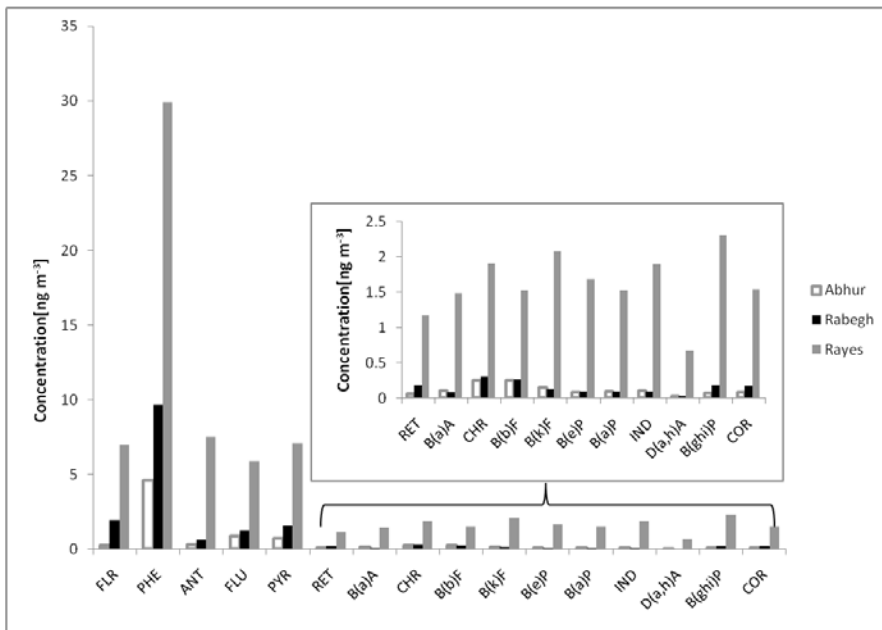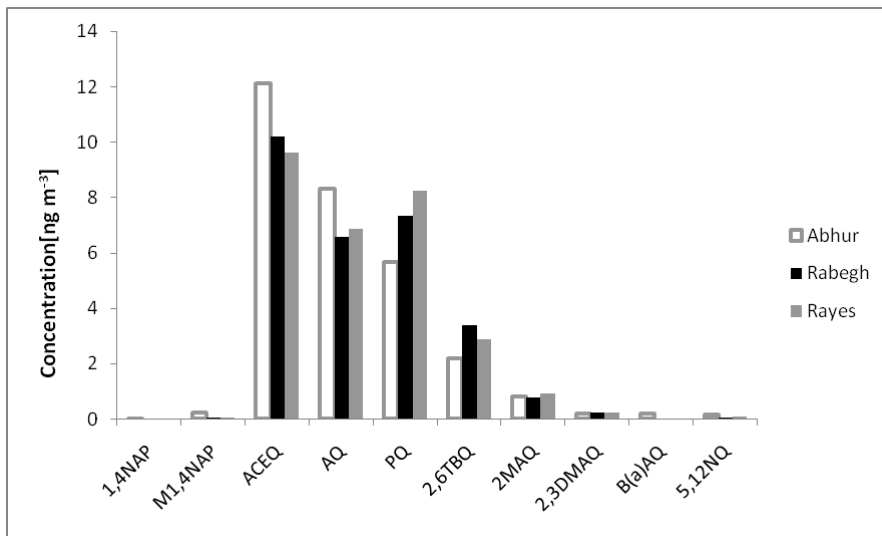
Figure 3: (a) Total PAH, (b) total oxy-PAH and (c) total nitro-PAH at the three sites on 29th September 2013.